J Therm Anal Calorim (2009) 97:721–727
DOI 10.1007/s10973-009-0280-4

New complexes of Ni(II) and Cu(II) with Schiff bases functionalised with 1,3,4-thiadiazole: spectral, magnetic, biological and thermal characterisation

Rodica Olar · Mihaela Badea · Dana Marinescu · Veronica Lazar · Carmen Chifiriuc

ICTAC2008 Conference

Abstract Schiff bases obtained by the condensation of 2-amino-5-mercapto-1,3,4-thiadiazole with 2,4-pentandione or 1-phenyl-1,3-butandione were synthesized and characterized in order to obtain polydentate ligands HL^1 and HL^2, respectively. The complexes with these ligands of the type $M(L)Cl \cdot nH_2O$ [(**1**) M:Ni, L:L^1, $n = 0.5$; (**3**) M:Ni, L:L^2, $n = 0.5$]; [(**2**) M:Cu, L:L^1, $n = 1$; (**4**) M:Cu, L:L^2, $n = 0$] were also synthesized and characterized. The modifications evidenced in IR spectra of complexes were correlated with the presence of monodeprotonate Schiff bases. The electronic spectra display the characteristic pattern of square-planar stereochemistry. The in vitro qualitative and quantitative antimicrobial activity assays showed that the new complexes exhibited variable antimicrobial activity. The thermal analyses have evidenced the thermal intervals of stability and also the thermodynamic effects that accompany them. Schiff bases and complexes have a similar thermal behaviour. Processes as water elimination, melting, chloride anion removal as well as oxidative degradation of the organic ligands were observed.

Keywords Complexes · Gram negative strain · Gram positive strain · Thermal behaviour · 1,3,4-thiadiazole

---

R. Olar (✉) · M. Badea · D. Marinescu
Faculty of Chemistry, Department of Inorganic Chemistry, University of Bucharest, 90-92 Panduri Str., 050663 Sector 5, Bucharest, Romania
e-mail: marioara.olar@unibuc.ro; rodica_m_olar@yahoo.com

V. Lazar · C. Chifiriuc
Faculty of Biology, Department of Microbiology, University of Bucharest, 1-3 Aleea Portocalilor Str., 060101 Sector 6, Bucharest, Romania

Introduction

Heterocycles bearing a 1,3,4-thiadiazole moiety, represent an interesting class of compounds displaying a wide spectrum of biological activities such as anti-inflammatory, antiviral, antitumor, antiulcer, antiepileptic as well as antimicrobial properties [1–3]. Some 1,3,4-thiadiazole derivatives are good inhibitors of matrixins and bacterial collagenases, enzymes which can degrade the tissue leading to a variety of diseases such as cancer, rheumatoid arthritis, multiple sclerosis, and congestive heart failure [4, 5]. Moreover, diversified Schiff bases derived from 1,3,4-thiadiazole have been obtained and the inhibitory properties toward Carbonic anhydrase [6] or antimicrobial activities both for these compounds and their complexes have been reported [6–9].

In order to evaluate the biological properties and thermal stability of such derivatives, we report here the synthesis and characterization of two Schiff bases obtained by the 2-amino-5-mercapto-1,3,4-thiadiazole condensation with 2,4-pentandione or 1-phenyl-1,3-butandione. The complexes of Ni(II) and Cu(II) with these ligands were also synthesized and characterised. The Schiff bases and complexes have been characterized by different analytical and spectral methods. The antimicrobial activity of these derivatives was also assayed against planktonic microbial strains.

The thermal behaviour of these derivatives was investigated in synthetic air by thermal analysis (TG, DTA). So far, our research group reported the thermal behaviour of other complexes with 1,3,4-thiadiazole derivatives [10–12]. The thermal behaviour of the complexes with other Schiff bases has attracted attention in the last years [13–20], this attention being focused on the species that could have some practical applications [15, 19, 20]. Data concerning kinetic studies were also reported for such type of compounds [15, 17–19].

Experimental

All reagents were of commercial analytical quality and have been used without further purification. Chemical analysis of carbon, nitrogen and hydrogen has been performed using a Perkin–Elmer PE 2400 analyzer. Nickel and chloride were determined gravimetrically using dimethylglyoxyme and silver nitrate, respectively, while copper was determined volumetrically using thiosulfate method in the laboratories of Inorganic Chemistry Department.

IR spectra were recorded in KBr pellets with a BIO-RAD FTIR 135 spectrometer in the range 400–4000 cm^{-1}. Electronic spectra by diffuse reflectance technique, with MgO as standard, were recorded in the range 280–2800 nm, on a Jasco V 670 spectrophotometer. Magnetic measurements were done by Faraday's method, at room temperature, using $Hg[Co(NCS)_4]$ as standard. The molar magnetic susceptibilities were calculated and corrected for the atomic diamagnetism. EPR spectra were recorded on microcrystalline samples at room temperature with a Varian E-9 spectrometer. The field was calibrated using crystalline diphenyilpicrylhydrazyl ($g = 2.0036$).

The qualitative screening of the susceptibility spectra of different microbial strains to the complexes was performed by adapted diffusion techniques, while the quantitative assay of minimal inhibitory concentration (MIC, $\mu g/cm^3$) value was based on liquid medium serial microdilutions [21]. The compounds were solubilised in DMF to a final concentration of 1 mg/mL. The in vitro biological screening effects were tested against a microbial inoculum of $\sim 1.5 \times 10^8$ UFC/cm^3, corresponding to 0.5 McFarland density, represented by *Enterobacteriaceae* (*E. coli*, *Salmonella* sp., *Shigella* sp., *Proteus* sp., *Klebsiella pneumoniae*) *Pseudomonadaceae* (*Pseudomonas aeruginosa*, *Acinetobacter boumani*), *Micrococcaceae* (*Staphylococcus aureus)*, *Bacillaceae* (*Bacillus* sp.), and *Candida* strains, reference ones and recently isolated from clinical samples.

The heating curves (TG and DTA) were recorded using a Labsys 1200 SETARAM instrument, with a sample mass of 6–17 mg over the temperature range of 20–1000 °C, using a heating rate of 10 K/min. The measurements were carried out in synthetic air atmosphere (flow rate 16.66 cm^3/min) by using alumina crucibles.

Synthesis of the complexes

The syntheses of Schiff bases were performed by heating for 4 h a mixture of 2-amino-5-mercapto-1,3,4-thiadiazole with 2,4-pentandione or 1-phenyl-1,3-butandione for molar ratio 1:1 in the presence of metal chloride. Structural data for Schiff bases will be presented elsewhere. These compounds were characterised by elemental analysis and IR data.

HL^1: IR (KBr pellet), cm^{-1}: $\nu_{as}(CH_3)$, 2962w; $\nu_s(CH_3)$, 2914w; TI (δ(NH) + ν(C=N) + δ(CH)), 1606s; (ν(C=C) + ν(C=N)), 1524m, 1369s; $\delta_{as}(CH_3)$, 1421w; TII (δ(NH) + δ(CH) + ν(C=N) + ν(C=S)), 1345vs; ν(C=C) + ν(C–CH), 1283w; ν(C–N), 1181m; TIII (ν(C=N) + ν(C=S)), 1053m; ν(N–N), 957m; δ(SH), 906w; TIV (ν(C=S)), 729w; ν_{as}(C–S–C), 647w; ν_s(C–S–C), 536w.

HL^2: IR (KBr pellet), cm^{-1}: ν(CH), 3068w; $\nu_{as}(CH_3)$, 2962w; $\nu_s(CH_3)$, 2914w; TI (δ(NH) + ν(C=N) + δ(CH)), 1596s; (ν(C=C) + ν(C=N)), 1514m, 1453w; $\delta_{as}(CH_3)$, 1416w; TII (δ(NH) + δ(CH) + ν(C=N) + ν(C=S)), 1337vs; ν(C=C) + ν(C–CH), 1266w; ν(C–N), 1210w; TIII (ν(C=N) + ν(C=S)), 1023m; δ(SH), 927w; γ(CH), 844w, 772w, 692w; TIV (ν(C=S)), 735w; ν_{as}(C–S–C), 637w; ν_s(C–S–C), 546w.

The complexes were obtained following the general procedure: to a solution of 5 mmol of MCl_2 in 50 mL ethanol was added drop wise at 50 °C, under continuous stirring, a solution of 5 mmol Schiff base in 20 mL ethanol. A solution of LiOH 1% was added drop wise until the solution turn yellow (for nickel) or brown (for copper). The yellow or brown, sparingly soluble compound formed after 1 h was filtered out and washed with ethanol and air dried.

$[Ni(L^1)Cl]\cdot 0.5H_2O$ (**1**): Analysis, found: Ni, 19.43; C, 27.93; Cl, 11.78; H, 2.86; N, 14.01; S, 21.23 $NiC_7ClH_8N_3O_{0.5}S_2$ requires: Ni, 19.53; C, 27.98; Cl, 11.80; H, 2.68; N, 13.98; S, 21.35; IR (KBr pellet), cm^{-1}: ν(OH), 3414w; $\nu_{as}(CH_3)$, 2960m; $\nu_s(CH_3)$, 2910m; TI (δ(NH) + ν(C=N) + δ(CH)), 1606s; (ν(C=C) + ν(C=N)), 1523m, 1385s; $\delta_{as}(CH_3)$, 1435m; TII (δ(NH) + δ(CH) + ν(C=N) + ν(C=S)), 1360vs; ν(C=C) + ν(C–CH), 1279s; ν(C–N), 1180m; TIII (ν(C=N) + ν(C=S)), 1054m; ν(N–N), 957m; TIV (ν(C=S)), 702w; ν_{as}(C–S–C), 660m; ν_s(C–S–C), 535w. UV–Vis (MgO pellet), cm^{-1}: $^1A_1 \rightarrow {}^1A_2$: 17543; μ_{eff}, μ_B: 0.

$[Cu(L^1)Cl]\cdot H_2O$ (**2**): Analysis, found: Cu, 20.18; C, 26.88; Cl, 11.38; H, 2.75; N, 13.37; S, 20.49 $CuC_7ClH_9N_3OS_2$ requires: Cu, 20.22; C, 26.75; Cl, 11.28; H, 2.89; N, 13.37; S, 20.41; IR (KBr pellet), cm^{-1}: ν(OH), 3450m; $\nu_{as}(CH_3)$, 2940m; $\nu_s(CH_3)$, 2890m; TI (δ(NH) + ν(C=N) + δ(CH)), 1610m; (ν(C=C) + ν(C=N)), 1530m, 1375s; $\delta_{as}(CH_3)$, 1435w; TII (δ(NH) + δ(CH) + ν(C=N) + ν(C=S)), 1355m; ν(C=C) + ν(C–CH), 1275w; ν(C–N), 1180w; TIII (ν(C=N) + ν(C=S)), 1055m; ν(N–N), 957m; TIV (ν(C=S)), 705w; ν_{as}(C–S–C), 660w; ν_s(C–S–C), 530w. UV–Vis (MgO pellet), cm^{-1}: CT: 28570; $d_{xy} \rightarrow d_{x2-y2}$: 16390; μ_{eff}, μ_B: 0.75.

$[Ni(L^2)Cl]\cdot 0.5H_2O$ (**3**): Analysis, found: Ni, 16.09; C, 39.77; Cl, 9.82; H, 2.81; N, 11.65; S, 17.69 $NiC_{12}ClH_{10}N_3O_{0.5}S_2$ requires: Ni, 16.15; C, 39.65; Cl, 9.75; H, 2.77; N, 11.56; S, 17.65; IR (KBr pellet), cm^{-1}: ν(OH), 3400m; ν(CH), 3080m; $\nu_{as}(CH_3)$, 2960m; $\nu_s(CH_3)$, 2930m; TI (δ(NH) + ν(C=N) + δ(CH)), 1600vs; (ν(C=C) + ν(C=N)), 1518vs, 1386m; $\delta_{as}(CH_3)$, 1420m; TII (δ(NH) + δ(CH) +

ν(C=N) + ν(C=S)), 1360s; ν(C=C) + ν(C–CH), 1290m; ν(C–N), 1185m; TIII (ν(C=N) + ν(C=S)), 1025vs; γ(CH), 840w, 720w, 690w; TIV (ν(C=S)), 730w; ν_{as}(C–S–C), 630w; ν_s(C–S–C), 560w. UV–Vis (MgO pellet), cm^{-1}: $^1A_1 \rightarrow {}^1A_2$: 17700; μ_{eff}, μ_B: 0.

[Cu(L^2)Cl] (**4**): Analysis, found: Cu, 17.68; C, 40.38; Cl, 9.91; H, 2.48; N, 11.74; S, 17.82 $CuC_{12}ClH_9N_3S_2$ requires: Cu, 17.73; C, 40.22; Cl, 9.89; H, 2.53; N, 11.73; S, 17.90; IR (KBr pellet), cm^{-1}: ν(CH), 3069m; ν_{as}(CH$_3$), 2960m; ν_s(CH$_3$), 2935m; TI (δ(NH) + ν(C=N) + δ(CH)), 1595s; (ν(C=C) + ν(C=N)), 1513m, 1384 m; δ_{as}(CH$_3$), 1410m; TII (δ(NH) + δ(CH) + ν(C=N) + ν(C=S)), 1350m; ν(C=C) + ν(C–CH), 1270w; ν(C–N), 1180w; TIII (ν(C=N) + ν(C=S)), 1040m; γ(CH), 844w, 720w, 690w; TIV (ν(C=S)), 726w; ν_{as}(C–S–C), 635w; ν_s(C–S–C), 550w. UV–Vis (MgO pellet), cm^{-1}: CT: 29410; $d_{xy} \rightarrow d_{x2-y2}$: 17857; μ_{eff}, μ_B: 1.29.

Results and discussions

Physico-chemical characterisation of complexes

In this article, we report the preparation, physico-chemical and biological characterisation of some Schiff bases (HL^1 and HL^2) resulted in 2-amino-5-mercapto-1,3,4-thiadiazole condensation with 2,4-pentandione or 1-phenyl-1, 3-butandione for 1:1 molar ratio. The structure of these compounds as resulted from X-ray determination is:

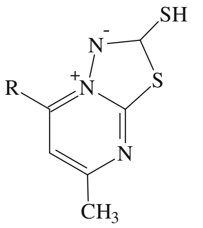

HL^1: R=CH$_3$;
HL^2: R=C$_6$H$_6$

The complexes M(L)Cl·nH$_2$O ((**1**) M:Ni, L:L^1, $n = 0.5$; (**3**) M:Ni, L:L^2, $n = 0.5$); ((**2**) M:Cu, L:L^1, $n = 1$; (**4**) M:Cu, L:L^2, $n = 0$) were also synthesized and characterised. The major goal of this article was to evidence the thermal behaviour of these Schiff base and their complexes that also present in vitro an antibacterial activity.

The major IR spectral features of complexes presented at experimental part indicate that the bands corresponding to the combined vibration modes of the thioamide group from the 1,3,4-thiadiazole moiety are present in the spectra of both ligands and complexes [22–24]. Also the bands due to amine group are absent in spectra of compounds according with the condensation processes. New bands appear in the region characteristic for the heterocyclic ν(C=C) + ν(C=N) vibrations [25].

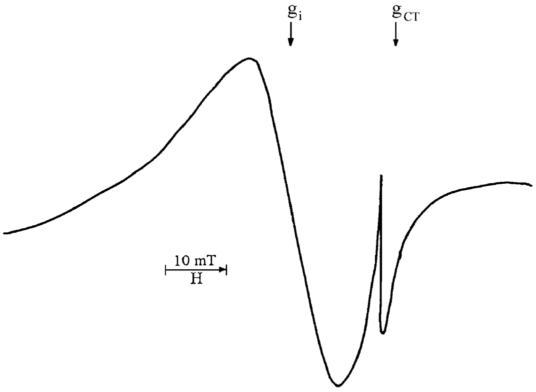

Fig. 1 X-band EPR spectrum of complex (**2**) on polycrystalline sample at room temperature

In the complexes spectra the bands assigned to TIII vibration mode are shifted towards lower wavenumbers. This behaviour indicates the mercapto group deprotonation of the and its involvement in coordination. In the characteristic ranges for water a large band about 3400 cm^{-1} for the complexes can be assigned to ν(OH) stretching vibrations, except for complex (**4**) [25].

The electronic spectra of compounds show the characteristic pattern of the square-planar stereochemistry. The bands about 17500 cm^{-1} are assigned to $^1A_1 \rightarrow {}^1A_2$ transition while the intense ones at higher energy are associated with charge transfer for Ni(II) compounds. The electronic spectra of Cu(II) complexes display a broad band centred at 16390/17857 cm^{-1} assigned to $d_{x2-y2} \rightarrow d_{xy}$ spin allowed transition [26].

The Ni(II) complexes are diamagnetic as is expected for a square planar specie. The EPR spectrum of complex (**2**) (Fig. 1) display a low intensity isotropic signal with a value of factor $g = 2.115$. Moreover, a second narrow signal with $g = 2.011$, value closer to the free electron one, have origin in a charge transfer metal to ligand.

Compound (**4**) is EPR silent suggesting the possibility of polymerisation and the appearance of an antiferromagnetic coupling between paramagnetic ions mediated by the bridging ligands. This behaviour is also according with the smaller value of the magnetic moment at room temperature.

The square planar surrounding of the M(II) centres are supposed to be realised through both chloride and sulphur bridges, assembling poly-nuclear entities in the solid state of the compound (as is shown below).

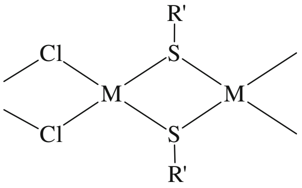

Biological activity

The antimicrobial activity of the tested compounds was performed against 15 microbial strains, the majority of them being recently isolated from different clinical samples and exhibiting different resistance patterns, i.e., *Enterobacteriaceae* (*E. coli*—enteropathogenic epec strains, as well as strains producing extended spectrum beta-lactamases-esbl rendering them resistant to all beta-lactams, *Salmonella* sp., *Shigella flexneri* and *Shigella* sp., *Proteus* sp., *Klebsiella pneumoniae*) *Pseudomonadaceae* (*Pseudomonas aeruginosa*, *Acinetobacter boumani*—both microorganisms being known for their high natural resistance to antibiotics), *Micrococcaceae* (*Staphylococcus aureus methicillin resistant—MRSA*), *Bacillaceae* (*Bacillus* sp.) and *Candida albicans* strains. The values of minimum inhibitory concentration (MIC, μg/mL) are presented in Fig. 2.

All tested compound exhibited good antimicrobial activity (with MIC values ranging from 32 to 256 μg/cm^3).

The new copper complexes presented the best antimicrobial activity against Gram-positive microorganisms, with an improved MIC comparing with the free ligand, i.e., complex (**2**) exhibited a MIC of 64 μg/mL against methicilin resistant *Staphylococcus* aureus while compound (**4**) display a similar MIC against *Bacillus subtilis*.

The antimicrobial activity of all four new complexes was superior comparatively to the free ligand in case of *Pseudomonas aeruginosa* and *Acinetobacter boumani* strains.

In exchange, the Schiff bases proved to be more or equally active comparatively with the new complexes against Gram-negative, enterobacterial and fungal strains.

It must be mentioned that the used solvent, DMF, do not influenced the antimicrobial activity of the tested compounds at the working concentrations.

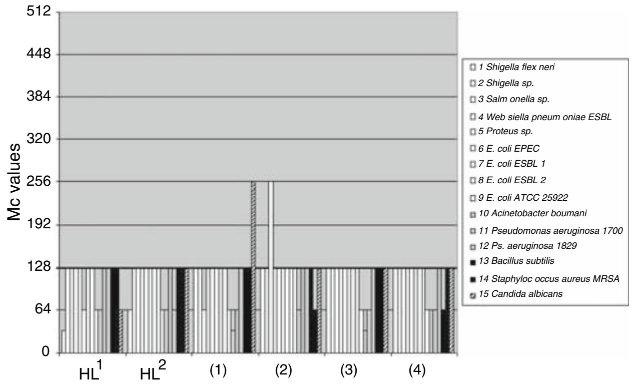

Fig. 2 The representation of the antimicrobial activity (MIC values) of the tested compounds (*white columns*—Gram negative, enterobacterial bacterial strains, *grey columns*—Gram negative, pseudomonade strains, *black columns*—Gram-positive bacterial strains, *dark upward diagonal columns*—*Candida albicans*)

The complexes were tested also in vitro for anti-HIV activity but it was not evidenced any significant activity. This behaviour could be assigned either to degeneration or rapid metabolisation of the complexes in the cultures conditions.

Thermal behaviour of complexes

The results concerning the thermal decomposition/degradation of the Schiff bases and complexes are presented in the following (Table 1).

Schiff bases display the same thermal behaviour and the general aspect of the DTA and TG curves excepting that the HL_1 melts at 210 °C, process that is not observed for HL_2 (Figs. 3, 4). This behaviour is consistent with a higher molar mass corresponding to HL_2.

Thermal decomposition follows in three exothermic steps. For HL_1, the melting is immediately followed by the thermal decomposition that starts in the first step with CS_2 elimination and preservation of the six-member ring resulted after condensation. The following steps are an overlapping of at least four processes as both TG and DTA indicates and corresponds with the gradually oxidative degradation of the remaining organic part. It is worth to be mentioned that the thermal decomposition is not finished at 1000 °C for HL_2, the graphite residue being identified in the crucible.

Thermal decomposition of $[Ni(L^1)Cl]\cdot 0.5H_2O$

The TG and DTA curves corresponding to the complex (**1**) heated in the 20–900 °C temperature range indicate that decomposition follows three steps (Fig. 5).

The first step of compound transformation consists in an endothermic elimination of water molecules (Table 1). The temperature range corresponding to the lost indicates their nature as crystallisation water. The anhydrous specie is stable over a 50 °C temperature range. The second step, exothermic, is not a single one being an overlap of at least two processes as both TG and DTA curves indicate. This step corresponds to the partial Schiff base oxidative degradation that leads to 2-mercapto-1,3,4-thiadiazolyl fragment that remain coordinated. This behaviour could be generated by the fact that monoanionic Schiff base is coordinated through exocyclic sulphur to metallic ion and this interaction stabilises the thiadiazole ring. Next step, exothermic also, corresponds to organic part oxidative degradation together with chloride loss. This consists in at least four processes (according to TG and DTA curves profile). The final product is NiO (found/calcd. overall mass loss: 75.2/75.1).

Table 1 Thermal behaviour data (in synthetic air atmosphere) for Schiff bases and complexes

Complex	Step	Thermal effect	Temperature range/°C	Δm_{exp}/%	Δm_{calc}/%
HL^1		Endothermic	210*	0	0
	1.	Strong exothermic	210–240	38.1	38.4
	2.	Exothermic	240–410	27.0	27.3
	3.	Exothermic	410–1000	34.8	34.3
HL^2	1.	Strong exothermic	194–280	29.2	29.3
	2.	Exothermic	280–890	44.8	45.0
	3.	Exothermic	890–1000	13.3	25.7
$[Ni(L^1)Cl]\cdot 0.5H_2O$	1.	Endothermic	70–130	2.9	3.0
	2.	Exothermic	170–320	26.8	26.6
	3.	Exothermic	320–900	45.4	45.5
	Residue NiO			24.8	24.9
$[Cu(L^1)Cl]\cdot H_2O$	1.	Endothermic	70–140	5.7	5.7
	2.	Exothermic	170–260	25.5	25.5
	3.	Exothermic	260–730	43.5	43.5
	Residue CuO			25.3	25.3
$[Ni(L^2)Cl]\cdot 0.5H_2O$	1.	Endothermic	70–130	2.5	2.5
	2.	Exothermic	180–430	39.3	39.4
	3.	Exothermic	430–800	37.6	37.6
	Residue NiO			20.5	20.6
$[Cu(L^2)Cl]$	1.	Exothermic	170–290	21.5	21.5
	2.	Exothermic	290–860	56.3	56.3
	Residue CuO			22.2	22.2

*melting point

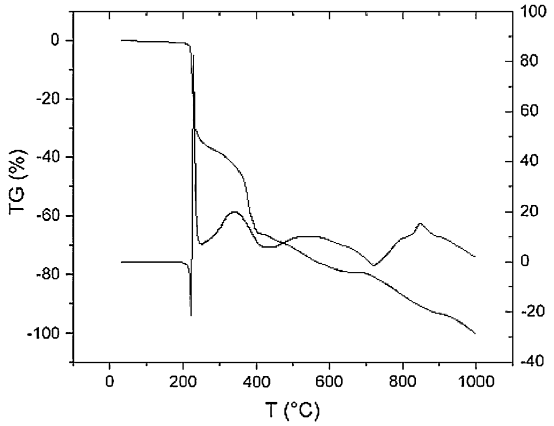

Fig. 3 TG and DTA curves of HL^1

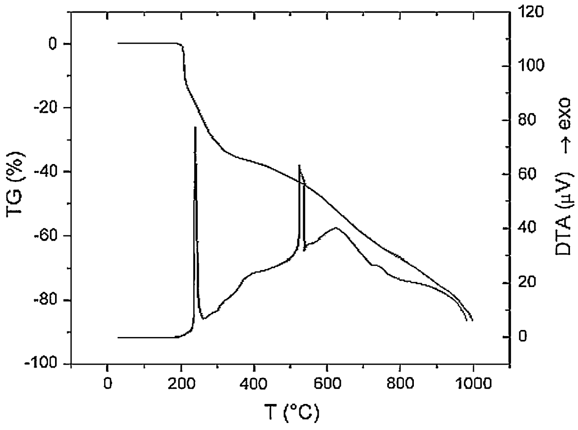

Fig. 4 TG and DTA curves of HL^2

Thermal decomposition of $[Cu(L^1)Cl]\cdot H_2O$

The decomposition of complex (**2**) comprises also three steps and starts with water elimination, process that also occurs at low temperatures (Fig. 6).

The anhydrous specie is stable over a 30 °C temperature range. The thermal degradation of this intermediate starts at 170 °C and comprises two steps. The second step occurs in two exothermic processes as both TG and DTA profile indicate. At least four processes (according to both TG and DTA) can be noticed in the last step. Finally, the oxidative degradation leads to CuO in accord with the overall mass loss (found/calcd: 74.6/74.7).

Thermal decomposition of $[Ni(L^2)Cl]\cdot 0.5H_2O$

According to the TG profile the decomposition of $[Ni(L_2)Cl]\cdot 0.5H_2O$ (**3**) occurs in three, well-defined steps (found/calcd. overall mass loss: 79.4/79.5) (Fig. 7).

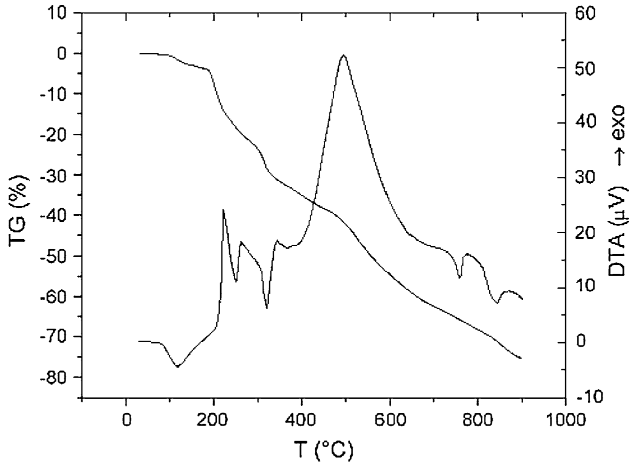

Fig. 5 TG and DTA curves of [Ni(L^1)Cl]·0.5H$_2$O

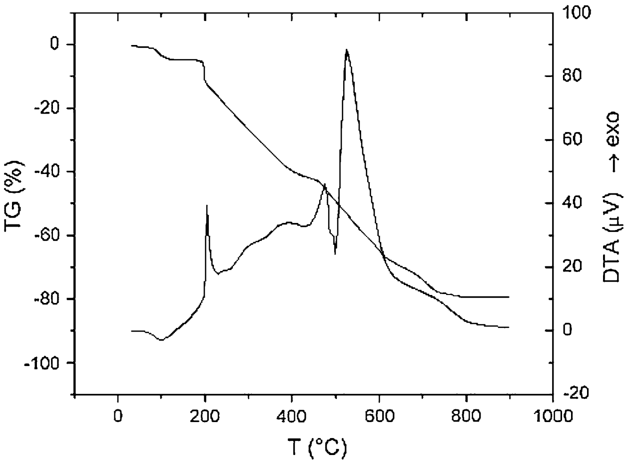

Fig. 7 TG and DTA curves of [Ni(L^2)Cl]·0.5H$_2$O

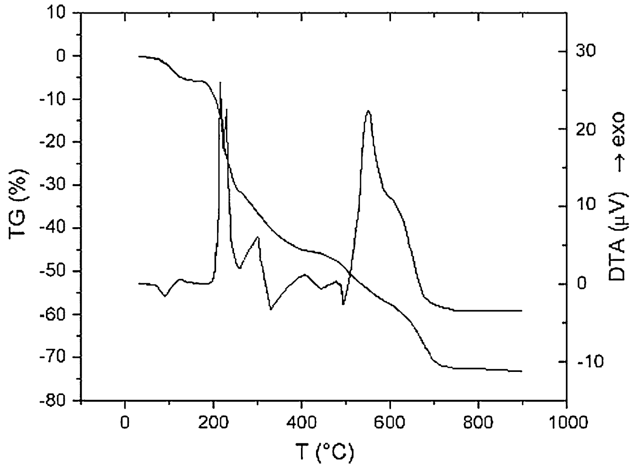

Fig. 6 TG and DTA curves of [Cu(L^1)Cl]·H$_2$O

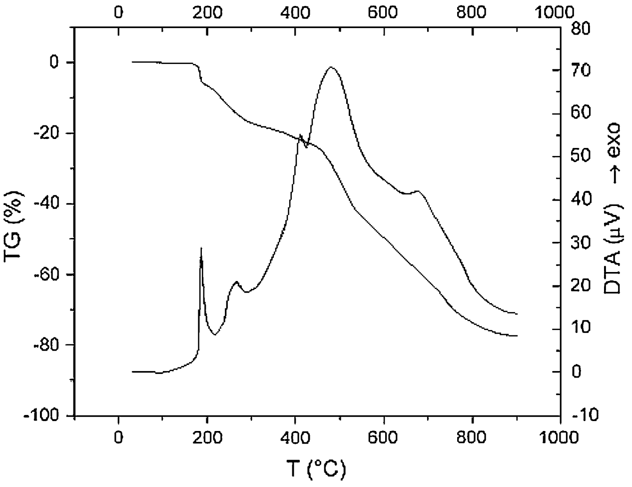

Fig. 8 TG and DTA curves of [Cu(L^2)Cl]

After water loss in the the 50–130 °C range, the anhydrous specie is stable over a 50 °C temperature range. The next step corresponds to the Schiff base partial oxidative degradation. According to mass loss the 2-mercapto-1,3,4-thiadiazolyl fragment remain also coordinated as result of stabilisation induced by the Ni(II). The step consists in at least two processes as both TG and DTA indicate. The chloride elimination together with the rest of organic part leads to NiO in the final step. The TG and DTA profiles are consistent with at least four processes.

Thermal decomposition of [Cu(L^2)Cl]

Complex (**4**) is anhydrous and as result is very stable up to 170 °C (Fig. 8). As a consequence the decomposition comprises only two steps and starts with the oxidative degradation of a part of the organic ligand. The mass loss corresponds to the benzene ring removal. For the first one the TG and DTA curves indicate two interfering processes. Next step comprises at least three processes (according to TG and DTA) and consists in the remaining organic fragment and chloride elimination. The final product is also CuO (found/calcd. overall mass loss: 77.8/77.8).

Conclusions

Two Schiff bases derived from 2-amino-5-mercapto-1,3,4-thiadiazole and the corresponding Ni(II) and Cu(II) complexes were characterised in order to obtain new effective antibacterial agents with a large spectrum of biological activity.

Electronic and EPR spectra of complexes are characteristic for a square planar stereochemistry. The modifications in the IR spectra of ligands are in accord with the condensation process. The low values of magnetic moments observed for Cu(II) complexes are an indicative of interaction between paramagnetic ions at room temperature.

The antimicrobial activity of all new complexes was superior comparatively to the free ligand in case of *Pseudomonas aeruginosa* and *Acinetobacter boumani* strains. The copper complexes presented the best antimicrobial activity against *Staphylococcus aureus* and *Bacillus subtilis* strains. In exchange, the free ligands proved to be more or equally active comparatively with the complexes against Gram-negative, enterobacterial and fungal strains.

Thermal decomposition of complexes allowed us to establish the number and nature of water molecule, the composition of complexes and also the intervals of thermal stability. The thermal degradation occurs in three steps for the organic derivatives and the HL^1 melting was observed before decomposition. After water elimination up to 140 °C, the complexes decompose in two steps leading at metal (II) oxides as final products. The results are in good concordance with the complexes composition.

Acknowledgements The VIASAN Romanian National Research Program 142/2006 financially supported this study.

References

1. Holla BS, Poojary KN, Rao BS, Shivanada MK. New bis-mercapto triazoles and bistriazolothiadiazoles as possible anticancer agents. Eur J Med Chem. 2002;37:511–7.
2. Swamy SN, Basappa G, Priya BJ, Prabhuswany B, Doreswamy BH, Prasad JS, et al. Synthesis of pharmaceutically important condensed heterocyclic 4,6-disubstituted-1,2,4-triazolo-1,3,4-thiadiazole derivatives as antimicrobials. Eur J Med Chem. 2006; 41:531–8.
3. Amir M, Kumar H, Javed SA. Synthesis and pharmacological evaluation of condensed heterocyclic 6-substituted-1,2, 4-triazolo[3,4-b]-1,3,4-thiadiazole derivatives of naproxen. Bioorg Med Chem Lett. 2007;17:4504–8.
4. Scozzafava A, Supuran CT. Protease inhibitors: synthesis of matrix metalloproteinase and bacterial collagenase inhibitors incorporating 5-amino-2-mercapto-1,3,4-thiadiazole zinc binding functions. Bioorg Med Chem Lett. 2002;12:2667–72.
5. Jamloki A, Karthikeyan C, Hari Narayana Moorthy NS, Trivedi P. Bioorg Med Chem Lett. 2006;16:3847–54.
6. Mastrolorenzo A, Scozzafava A, Supuran CT. Antifungal activity of Ag(I) and Zn(II) complexes of aminobenzolamide (5-sulfanilylamido-1,3,4-thiadiazole-2-sulfonamide) derivatives. J Enzyme Inhib. 2000;15:517–31.
7. Chohan ZH, Pervez H, Rauf A, Scozzafava A, Supuran CT. Antibacterial Co(II), Cu(II), Ni(II) and Zn(II) complexes of thiadiazole derived furanyl, thiophenyl and pyrrolyl Schiff base. J Enzyme Inhib Med Chem. 2002;17:117–22.
8. Chohan ZH, Pervez H, Rauf A, Supuran CT. Antibacterial role of SO(4), NO(3), C(2)O(4) and CH(3)CO(2) anions on Cu(II) and Zn(II) complexes of a thiadiazole-derived pyrrolyl Schiff base. Met Based Drugs. 2002;8:263–7.
9. Chohan ZH, Scozzafava A, Supuran CT. Unsymmetrical 1,1′-disubstituted ferrocenes: synthesis of Co(II), Cu(II), Ni(II) and Zn(II) chelates of ferrocenyl-1-thiadiazolo-1′-tetrazole, -1-thiadiazolo-1′-triazole and -1-tetrazolo-1′-triazole with antimicrobial properties. J Enzyme Inhib Med Chem. 2002;17:261–6.
10. Badea M, Olar R, Brezeanu M, Marinescu D, Segal E. Thermal stability and non-isothermal kinetic study of three coordination compounds of Cu(II). Thermochim Acta. 1996;279:183–90.
11. Badea M, Olar R, Cristurean E, Marinescu D, Brezeanu M, Calina-Soradi C, et al. Thermal stability and non-isothermal decomposition kinetics. Heteropolynuclear compounds of Cu(II). J Therm Anal Calorim. 2000;59:977–84.
12. Olar R, Badea M, Stanica N, Cristurean E, Marinescu D. Synthesis, characterisation and thermal behaviour of some complexes with ligands having 1,3,4-thiadiazole moieties. J Therm Anal Calorim. 2005;82:417–22.
13. Konstantinoviæ SS, Radovanoviæ BC, Krklješ A. Thermal behaviour of Co(II), Ni(II), Cu(II), Zn(II), Hg(II) and Pd(II) complexes with isatin-â-thiosemicarbazone. J Therm Anal Calorim. 2007;90:525–31.
14. Abou El-Enein SA. Polymeric and sandwich Schiff's bases complexes derived from 4,4′-methylenedianiline: characterization and thermal investigation. J Therm Anal Calorim. 2008;91: 929–36.
15. Issa RM, Amer SA, Mansour IA, Abdel-Monsef AI. Thermal studies of bis salicylidene adipic dihydrazone derivatives and their complexes with divalent ions of Mn, Co, Ni, Cu and Zn. J Therm Anal Calorim. 2007;90:261–7.
16. Aksu M, Durmus S, Sari M, Emregül KC, Svoboda I, Fuess H, et al. Investigation on the thermal decomposition some hetero-dinuclear NiII–MII complexes prepared from ONNO type reduced Schiff base compounds (MII=ZnII, CdII). J Therm Anal Calorim. 2007;90:541–7.
17. Modi CK, Patel MN. Synthetic, spectroscopic and thermal aspects of some heterochelates. J Therm Anal Calorim. 2008;94: 247–55.
18. Patel SH, Pansuriya PB, Chhasatia MR, Parekh HM, Patel MN. Coordination chain polymeric assemblies of trivalent lanthanides with multidentate Schiff base synthetic, spectral investigation and thermal aspects. J Therm Anal Calorim. 2008;91:413–8.
19. Fan YH, Gao ZX, Bi CF, Xie ST, Zhang X. Synthesis and thermal decomposition kinetics of La(III) complex with unsymmetrical Schiff base ligand. J Therm Anal Calorim. 2008;91: 919–23.
20. Lalia-Kantouri M, Tzavellas L, Paschalidis D. Novel lanthanide complexes with di-2-pyridyl ketone-p-chlorobenzoylhydrazone: thermal investigation by simultaneous TG/DTG-DTA and IR spectroscopy. J Therm Anal Calorim. 2008;91:937–42.
21. Balotescu M-C, Oprea E, Petrache L-M, Bleotu C, Lazar V. Antibacterial, antifungal and cytotoxic activity of Salvia officinalis essential oil and tinctures. Roum Biotech Lett. 2005;10: 2481–9.
22. Gajendragad NR, Agarwala U. Complexing behaviour of 1,3,4-thiadiazole-2-thiol-5-amino-I. J Inorg Nucl Chem. 1975;37: 2429–34.
23. Gajendragad NR, Agarwala U. Complexing behaviour of 5-amino-1,3,4-thiadiazole-2-thiol. II. Complexes of Ni(II), Rh(I), Pd(II), Pt(II), Au(III) and Cu(II). Bull Chem Soc Jpn. 1975;48: 1024–9.
24. Gajendragad NR, Agarwala U. Complexing behaviour of 5-amino-2-thiol-1,3,4-thiadiazole-: Part III—complexes of Cu(I), Zn(II), Ag(I), Cd(II), Tl(I), Pb(II), Pd(0) and Pt(0). Ind Chem Soc. 1975;13:1331–4.
25. Nakamoto K. Infrared and Raman spectra of inorganic and coordination compounds. New York: Wiley; 1986. p. 207–27.
26. Lever ABP. Inorganic electronic spectroscopy. Amsterdam, London, New York: Elsevier; 1986. p. 507–54.